Structural Engineering and Mechanics, Vol. 10, No. 6 (2000) 635-650
DOI: http://dx.doi.org/10.12989/sem.2000.10.6.635

Adaptive nodal generation with the element-free Galerkin method

Heung-Jin Chung†

Department of Civil and Environmental Engineering, Jeonju University, Chonju 560-759, Korea

Gye-Hee Lee‡ and Chang-Koon Choi‡†

Department of Civil Engineering, KAIST, Taejon 305-600, Korea

Abstract. In this paper, the adaptive nodal generation procedure based on the estimated local and global error in the element-free Galerkin (EFG) method is proposed. To investigate the possibility of *h*-type adaptivity of EFG method, a simple nodal refinement scheme is used. By adding new node along the background cell that is used in numerical integration, both of the local and global errors can be controlled adaptively. These errors are estimated by calculating the difference between the values of the projected stresses and original EFG stresses. The ultimate goal of this study is to develop the reliable nodal generator based on the local and global errors that is estimated posteriori. To evaluate the performance of proposed adaptive procedure, the convergence behavior is investigated for several examples.

Key words: element-free Galerkin method; projection method; error estimation; adaptive analysis; intigration cell; nodal generation; refinement.

1. Introduction

In recent years, there have been efforts to develop new computational methods, so called meshless methods through modifying the basic structure of the traditional finite element method to make it more flexible and robust. These methods are very attractive for the development of adaptive methods of an *h*-type because nodes can easily be added or deleted and there is no need to generate a new element structure with the rearrangement or change in the number of nodes. In meshless methods, nodes can be located almost anywhere in the model or the entire array of nodes can be regenerated. Thus the need for generating a new mesh with adjustment of nodal locations and change in the number of nodes is avoided.

A reliable estimation of the error and an efficient distribution of nodes are crucial issues for the development of adaptive procedure for meshless method. Considerable effort has been devoted to these issues and indeed, significant advances have been achieved for some meshless method. Several adaptive methods and error estimates for meshless method have been proposed. Duarte and Oden (1996) derived an error estimate that involves only the computation of interior residuals and

† Assistant Professor
‡ Graduate Student
‡† Institute Chair Professor

the residuals where Neumann boundary conditions for the *h-p* cloud method. Liu *et al*. (1996) developed an adaptive algorithm from the edge detection technique for Reproducing Kernel Particle Methods (RKPM). Haussler-Combe and Korn (1998) proposed an adaptive procedure for element-free Galerkin (EFG) method which incorporates strain gradient and nodal distance.

In this study, we use an error criterion for deriving adaptivity in a meshless method based on moving least square (MLS) approximations described by Lancaster and Salkauskas (1981) is used. the implementation of the meshless method used here is the element-free Galerkin (EFG) method described in Belytschko, *et al*. (1994). EFG is related to the diffuse element method (Nayroles *et al*., 1992), but it is consistent in the sense that it passes the patch test, where DEM does not. In these methods, the approximation is obtained by a weighted least square fit to a set of nodal parameters. The weight functions are non-zero only over a small sub-domain; this sub-domain is called the compact support or the domain of influence.

It is well known that the stresses (or derivatives) calculated in finite element method (FEM) do not possess inter-element continuity and have a low accuracy at nodes and element boundaries. Many researchers proposed various continuous stress fields defined by shape functions and smoothed nodal parameters to obtain more accurate distribution of stresses. In FEM, *a posteriori* error can be estimated by comparing this smoothed stresses with FE stresses. In the EFG method, since there is no element, there is no inter-element discontinuity; that is, stress field is already smooth. Therefore stress smoothing techniques which work well in FEM are no longer effective in error estimation of EFG method. Since the exact values of interpolation error is not available in most cases, error can be estimated by calculating the difference between the values of the projected stress and those given directly by the EFG solution. Stress projection can be performed by taking product of shape function based on different domain of influence with the stresses at nodes.

Many researchers have proposed *h*-refinement schemes for meshless methods through adding nodes. Some of them are suitable to a certain condition like crack tip and have lack of flexibility for general analysis model. One of preferable refinement schemes is the use of background cell because it can maintain the suitable integration accuracy as the nodal density in local area increase. In this study, a simple adaptive nodal refinement scheme based on estimated error distribution is proposed to investigate the possibility of *h*-type adaptivity of EFG method. By adding new nodes along the background cell used in the numerical integration, both of the local and global errors that come from interpolation can be adaptively controlled. The ultimate goal of this study is to develop the reliable nodal generator based on the local and global errors that are estimated *posteriori*.

The paper is organized as follows. In section 2 the basic equations of the EFG approximation in elastostatics and the concept of a *posteriori* error estimation in EFG method are given. Section 3 describes the error criterion and adaptive refinement strategy. In section 4, the reliability and performance of adaptivity procedure proposed in this study are demonstrated in several two dimensional problems in which some singularities are included. Conclusions are stated in section 5.

2. EFG approximation and *a Posteriori* error estimation

2.1. EFG Approximation

In the moving least square technique, the local approximation $u_L^h(\boldsymbol{x})$ of the function $u(\boldsymbol{x})$ is expressed as the inner product of a vector of the polynomial basis $\boldsymbol{p}(\boldsymbol{x})$ and a vector of the

coefficients $\boldsymbol{a}(\boldsymbol{x})$

$$u_L^h(\boldsymbol{x}, \bar{\boldsymbol{x}})=\boldsymbol{p}^{\boldsymbol{T}}(\bar{\boldsymbol{x}})\boldsymbol{a}(\boldsymbol{x}) \tag{1}$$

where

$$\boldsymbol{x} \in \Omega_x,\ \boldsymbol{p}(\boldsymbol{x}) \in \boldsymbol{R}^m,\ \boldsymbol{p}(\boldsymbol{x}) \in \boldsymbol{R}^m$$

and m is the number of monomials in the polynomial basis. Using the MLS technique the vector $\boldsymbol{a}(\boldsymbol{x})$ can be obtained by minimizing the difference between the local approximation and the nodal values:

$$E[\boldsymbol{a}(\boldsymbol{x})]=\sum_{I=1}^{n} w_I(\boldsymbol{x}, a)[u_I - u_L^h(\boldsymbol{x}, \boldsymbol{x}_I)]^2=\sum_{I=1}^{n} w_I(\boldsymbol{x}, a)[u_I - \boldsymbol{p}^T(\boldsymbol{x}_I)\boldsymbol{a}(\boldsymbol{x})]^2 \quad \boldsymbol{x}_I \in \Omega_x \tag{2}$$

In the above, n is the number of nodes in Ω_x and $w_I(\boldsymbol{x}, a)=x(\boldsymbol{x}-\boldsymbol{x}_I, a)$ is a positive weighting function with compact support Ω_I of measure a; the compact support correspond to the domain of influence of the weight function. The following weight function have been used in this study.

$$w_I(\boldsymbol{x}, a)=\begin{cases} \dfrac{e^{-(d_I/c)^2}-e^{-(a/c)^2}}{(1-e^{-(a/c)^2})} & \text{if } d_I \le a \\ 0 & \text{if } d_I > a \end{cases} \tag{3a}$$

where c is a constant which controls the relative weights and $d_I=\|\boldsymbol{x}-\boldsymbol{x}_I\|$. Later, the domain of influence will be related to the mesh spacing

$$a=D_m h \tag{3b}$$

where h is the average nodal spacing.

The stationarity of $\boldsymbol{E}(\boldsymbol{a})$ with respect to $\boldsymbol{a}$ leads to:

$$\boldsymbol{a}(\boldsymbol{x})=\boldsymbol{A}^{-1}(\boldsymbol{x}, a)\boldsymbol{B}(\boldsymbol{x}, a)\boldsymbol{u} \tag{4a}$$

where

$$\boldsymbol{A}(\boldsymbol{x}, a)=\boldsymbol{p}^T(\boldsymbol{x}_I)w_I(\boldsymbol{x}, a)\boldsymbol{p}(\boldsymbol{x}_I) \tag{4b}$$

$$\boldsymbol{B}(\boldsymbol{x}, a)=\boldsymbol{p}^T(\boldsymbol{x}_I)w_I(\boldsymbol{x}, a) \tag{4c}$$

Letting the global approximation be related to the local approximation by

$$u^h(\boldsymbol{x})=u_L^h(\boldsymbol{x}, \bar{\boldsymbol{x}}) \tag{5}$$

and substituting Eq. (3) into Eq. (1) gives

$$u^h(\boldsymbol{x})=\boldsymbol{p}^{\boldsymbol{T}}(\boldsymbol{x})\boldsymbol{A}^{-1}(\boldsymbol{x})\boldsymbol{B}(\boldsymbol{x})\boldsymbol{u}\sum_{I}^{n}\sum_{j}^{m} p_j(x)(\boldsymbol{A}^{-1}(x)\boldsymbol{B}(x))_{jI}u_I \equiv \sum_{I}^{n}\phi_I(x)u_I \tag{6}$$

Eq. (6) is the MLS interpolant for $u(\boldsymbol{x})$.

2.2. Posteriori error estimation

To illustrate the basic ideas and implementation of the stress projetion, linear elasticity is considered.

The governing equation for elastostatics is

$$\boldsymbol{L}\boldsymbol{u} \equiv \boldsymbol{S}^T\boldsymbol{D}\boldsymbol{S}\boldsymbol{u}=\boldsymbol{f} \text{ in } \Omega \tag{7}$$

where $\boldsymbol{D}$ is the elasticity matrix and $\boldsymbol{S}$ is the differential operator which defines the strain as

$$\varepsilon^h(\boldsymbol{x})=\boldsymbol{S}\boldsymbol{u}^h(\boldsymbol{x}) \tag{8}$$

The directly computed stresses are

$$\sigma^h(\boldsymbol{x})=\boldsymbol{D}\sum_I^n \boldsymbol{S}\phi_I(x)\boldsymbol{u}_I \tag{9}$$

where n is the number of nodes in domain of influence for analysis; Ω_x^a. Appropriate boundary conditions are imposed on $\partial\Omega$.

An estimate of the derivative of a function $u(x)$ at any point $\boldsymbol{x} \in \Omega$ can be obtained by considering $\boldsymbol{a}(\boldsymbol{x})$ as a constant (Nayroles *et al.* 1992)

$$u^h_{,i} \approx \boldsymbol{p}_{,i}(\boldsymbol{x})\boldsymbol{a}(\boldsymbol{x}) \tag{10}$$

For accurate results, the coefficient $\boldsymbol{a}(\boldsymbol{x})$ should not be assumed to be constants. Belytschko *et al.* (1994) showed that not accounting for the spatial variation of $\boldsymbol{a}(\boldsymbol{x})$ detracts significantly from the accuracy of the method and results in failure to pass the patch test. They proposed a more accurate formula to calculate $u^h_{,i}$ as follows:

$$u^h_{,i}=\sum_I^n \phi_{I,i}(\boldsymbol{x})u_I=\sum_I^n \sum_j^m \{p_{j,i}(\boldsymbol{A}^{-1}\boldsymbol{B})_{iI} + p_j(\boldsymbol{A}^{-1}_{,i}\boldsymbol{B} + \boldsymbol{A}^{-1}\boldsymbol{B}_{,i})_{jI}\}u_I \tag{11}$$

where the index following a comma is a spatial derivative. The faster ways of computing the derivatives have been given in Belytschko *et al.* (1996a).

The frequency content of derivatives of the shape function is higher than that of shape function themselves. For this reason, more accurate results can be obtained for areas with high stress gradients, such as at a crack tip. However, these high frequencies in the derivatives of shape functions also introduce spurious oscillations at high gradient stress regions or discontinuous regions.

Chung and Belytschko (1998) proposed very simple and robust *posteriori* error estimate. The essence of the error estimate is to use the difference between the values of projected stresses $\boldsymbol{\sigma}^p$ and these given directly by the EFG method solution $\boldsymbol{\sigma}^h$. The projected stress is obtained by using an approximation with a different domain of influence. These projected stresses can be obtained as follows

$$\sigma^p(\boldsymbol{x})=\sum_K^l \left\{ \psi_K(\boldsymbol{x})\boldsymbol{D}\sum_I^n \boldsymbol{S}\phi_I(\boldsymbol{x}_K)\boldsymbol{u}_I \right\}=\sum_K^l \psi_K(\boldsymbol{x})\sigma^h(\boldsymbol{x}_K) \tag{12}$$

where $\sigma^h(\boldsymbol{x}_K)$ is the stress at node K, l is the number of nodes in domain of influence for projection Ω_x^p and $\psi_K(\boldsymbol{x})$ is an EFG shape function obtained with a different domain of influence. Thus the two shape functions are given as

$$\phi_I(\boldsymbol{x})=\sum_j^m p_j(\boldsymbol{x})(\boldsymbol{A}^{-1}(\boldsymbol{x}, a_1)\boldsymbol{B}(\boldsymbol{x}, a_1))_{jI} \tag{13}$$

$$\psi_K(\boldsymbol{x})=\sum_j^m p_j(\boldsymbol{x})(\boldsymbol{A}_p^{-1}(\boldsymbol{x}, a_2)\boldsymbol{B}_p(\boldsymbol{x}, a_2))_{jK} \tag{14}$$

with $a_1 \neq a_2$. To calculate $(\boldsymbol{A}_p^{-1}(\boldsymbol{x}, a_2)\boldsymbol{B}_p(\boldsymbol{x}, a_2))_{jK}$, the same procedure is used as before, i.e., Eqs. (1-6), but the domain of influence is reduced. The projected stress is computed simply by taking the product of shape function and stress computed at the nodes which are in the domain of influence of the point $\boldsymbol{x}$ considered Ω_x^p. The procedure is therefore quite inexpensive since there is no matrix solution procedure which is needed in most error estimation procedure.

Chung and Belytschko (1998) found in their numerical experiments that the error was estimated with accuracy when the domain of influence used for computing the projected stresses is close to the minimum size which preserves regularity of the moment matrix.

A measure of the pointwise error $\boldsymbol{\sigma}^e$ can be obtained at any point x in the solution domain as follows:

$$\boldsymbol{\sigma}^e(\boldsymbol{x}) = \boldsymbol{\sigma}^p(\boldsymbol{x}) - \boldsymbol{\sigma}^h(\boldsymbol{x}) \tag{15}$$

This error can be used as an indicator for adaptive analysis stated in next section.

3. Error criteria and adaptive refinement strategy

In general, adaptive procedures have a refinement criteria for local enrichment and a stop criteria for completeness of the procedure. To determine whether the enrichment through adding nodes is needed at a certain local domain, the approximation error need to be estimated locally. At the same time, to assess whether the accuracy of EFG solutions reaches a desired level at a global manner, the relative error estimator for solution domain is also needed.

To use point-wise error defined by Eq. (15) in consistent manner, the error should be evaluated in any appropriate norm. In this study, to measure the local error for each integration cell and the global error for whole solution domain, an energy norm is used. The point-wise error at a quadrature point, $x=x_g$ can be measured as follows:

$$\|e(\boldsymbol{x}_g)\| = \left\{ \frac{1}{2} \boldsymbol{\sigma}^{eT}(\boldsymbol{x}_g) \boldsymbol{D}^{-1} \boldsymbol{\sigma}^e(\boldsymbol{x}_g) \right\}^{1/2} \tag{16}$$

where subscript g indicates Gauss point. The approximation of the interpolation error in the energy norm for the whole solution domain Ω and for each background cell Ω_i can be calculated as

$$\|E\| = \left\{ \frac{1}{2} \int_{\Omega} \sigma^{eT}(\boldsymbol{x}) \boldsymbol{D}^{-1} \sigma^e(\boldsymbol{x}) d\Omega \right\}^{1/2} \tag{17}$$

and

$$\|E_i\| = \left\{ \frac{1}{2} \int_{\Omega_i} \sigma^{eT}(\boldsymbol{x}) \boldsymbol{D}^{-1} \sigma^e(\boldsymbol{x}) d\Omega \right\}^{1/2} \tag{18}$$

Above equations are known as the global and local error estimator, respectively. The local error indicator that is the refinement criteria for the cell i is calculated as

$$\eta_i = \left\{ \frac{\|E_i\|^2}{\|U\|^2 / Ncell} \right\}^{1/2} \tag{19}$$

where

$$\|U\| = \left\{ \frac{1}{2} \int_{\Omega} \sigma^{T}(\boldsymbol{x}) \boldsymbol{D}^{-1} \sigma(\boldsymbol{x}) d\Omega \right\}^{1/2} \tag{20}$$

If the estimated local error for the cell i is greater than the local error indicator, the cell i need to be refined adaptively through adding nodes, that is the background cell i is divided into four integration cells and five new nodes are added (Fig. 1). In the next step, it is checked whether added nodes are duplicated with existing nodes and reset the boundary conditions for new nodes. This procedure is repeated for each cell. After the refinement, the reanalysis is performed with new nodal configuration.

Liu *et al*. (1997) proposed similar refinement algorithm. Since they used high gradient nodes as a refinement indicator, special consideration for the cells with less than four nodes was needed. Besides, in this study estimation of local error and refinement procedure is based on integration cell, additional treatment for divided cell is not need throughout the refinement process.

At this point, it is worth to note the difference between the traditional finite element analysis and EFG method in adaptive *h*-refinement. In past decades, the adaptive mesh refinement technique along with an error analysis has been widely studied in the traditional FEM. The original isoparametric element with fixed number of nodes are commonly used in the past with displacement constraints imposed for inter-element compatibility. It is, however, inconvenient to refine the mesh locally at certain parts of the structure by using these types of elements only. When a refinement is performed, since the newly generated finite element mesh should satisfy the nodal connectivity of element, special elements to connect two different element layers are needed as transition elements (C.K. Choi *et al*. 1998, 1999).

In meshless methods, the discretization is based only on a set of nodes and does not require a mesh. The connectivity or the interaction of nodes is not fixed by input data, it need to be computed according to the nodal configuration. It is then possible to develop new nodal configuration of the model from a set of nodes and a description of boundary conditions. Therefore, there is no need to apply the special treatment or element to ensure the connectivity of newly developed degrees of freedom in meshless methods, where adaptive finite element method does.

Meanwhile, it should be noticed that there is still an open question with the integration order for each cell; what orders are needed to obtain an accurate quadrature result. Belytschko *et al*. (1994) recommended the following equation based on numerical experiences.

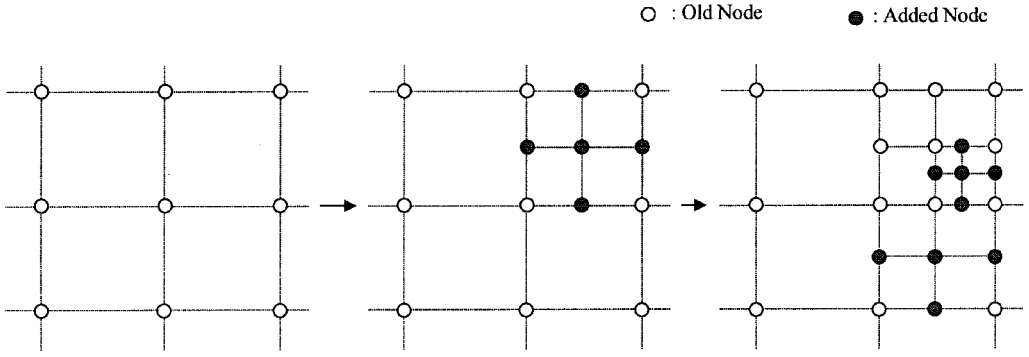

Fig. 1 Adaptive generation of new nodes and cells

$$N_q = \sqrt{M_c} + 2 \tag{21}$$

where N_q is the integration order and M_c is the number of nodes included in a cell area. This recommendation is confirmed by Haussler-Combe and Korn (1998). According to this recommendation, the order of quadrature for integration of a cell to which new nodes are added need to be modified properly. To avoid the abrupt change of integration resolution and retain the consistent quadrature accuracy, there would be two methods available. The first method is to increase the order of quadrature for cells with newly added nodes and the other one is to divide the integration cells. In

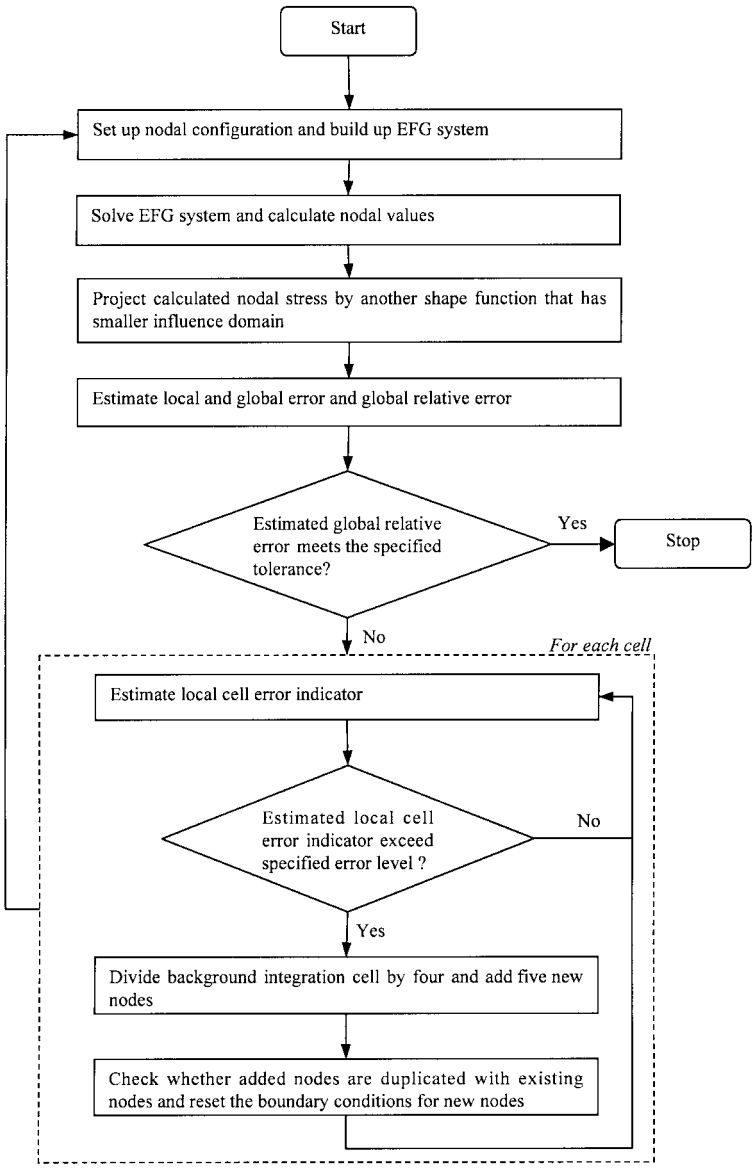

Fig. 2 Flow of analysis

this study, since nodes should be located along the background cell, the second method is more convenient to adopt.

The adaptive procedure will be continued until the specified error tolerances are met, i.e. the estimated relative error is smaller than the user defined level of accuracy. The relative error in the energy norm is defined by

$$R=\frac{\|E\|}{\|U\|} \tag{22}$$

If Eq. (22) is smaller than the prescribed tolerance, the procedure will be terminated.

The proposed adaptive refinement procedure is illustrated through the flow chart shown in Fig. 2.

4. Numerical Examples

The performance of the proposed adaptive procedure is demonstrated in two-dimensional examples that include *L*-shaped plate, the near-tip crack field problem and the edge crack problem. For all computations, the exponential weight function and a linear basis are used. The background cells were used for quadrature of the Galerkin terms such as the stiffness matrix with 5 by 5 Gauss quadrature in each cell.

In this numerical examples, the domain of influence, a_I, of a point x_I is determined as

$$a_I=D_m c_I \tag{23}$$

where D_m is a parameter of domain of influence and c_I is the characteristic dimension of the nodal spacing and is chosen as the distance to the third nearest neighbor node. The examples are analyzed with different parameters of D_m^p for projection and D_m^a for analysis.

4.1. Example 1: L-shaped plate

Fig. 3 shows an *L*-shaped plate subjected to a shear force on the top. Due to its shape, the stress concentration is occurred at concave corner. To deal with the corner, the imaginary crack line inclined for 45^o at the corner is assumed. This example is analyzed with the D_m^a =2.5 and D_m^p =1.75. In this example, the cell error indicator for refinement is 10%, except for the first iteration. The coarse nodal distribution of the first iteration can make an incorrect refinement trend. So a stricter cell error indicator of 5% for refinement is imposed at the first iteration stage. As the iteration continues, the adaptive and uniform refinement sequence of this problem is shown in Fig. 4 and *R* is relative error. As expected, the occurrence of refinement is concentrated around the concave edge which has steep gradient of stresses.

The convergence paths for adaptive and uniform refinement are shown in Fig. 5. In this figure, convergence curves show almost the same rate at the beginning of sequence. But, as the number of nodes increase, the difference of the performance between the adaptive refinement case and the uniform refinement case grows significantly.

4.2. Example 2. Near-tip crack field

The problem of a small plate with an edge crack subjected to the traction prescribed by the near

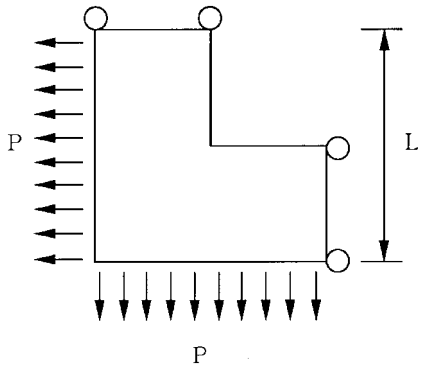

Fig. 3 L-shaped plate

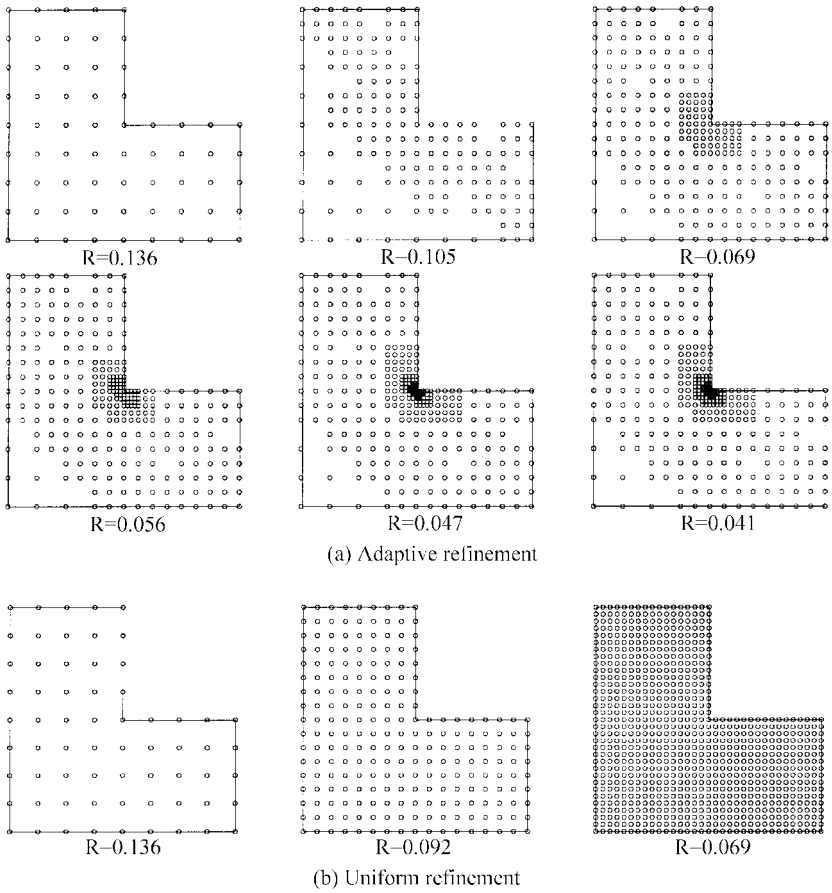

Fig. 4 Analysis sequences with relative error for example 1

field solution was considered. When a crack in a body is modeled, the displacement must be discontinuous across the crack. The method for construction of approximations around the tip of a discontinuity is the diffraction method (Belytschko *et al*. 1996a and Organ *et al*. 1996). This method

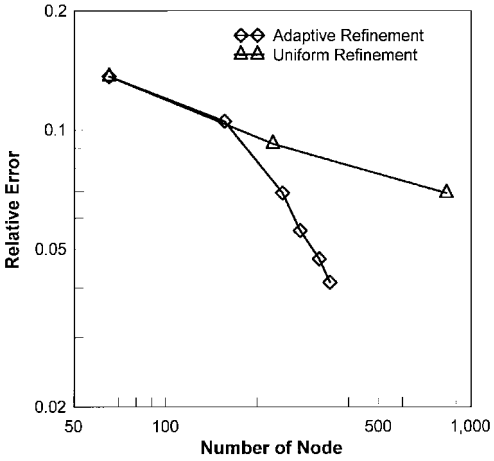

Fig. 5 Convergence curves for example 1

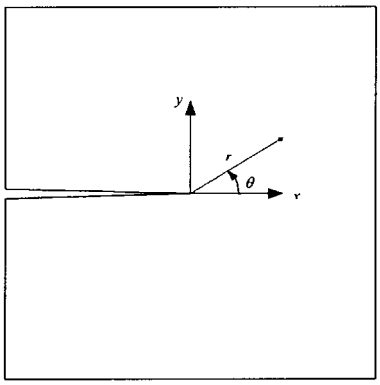

Fig. 6 Local coordinate system for near crack tip problem

treats the line of discontinuity as opaque but bases the weight function parameter on the length of the path which passes around the corner of discontinuity.

A closed form displacement solution of near-tip crack field can be written as Eqs (24). A square patch with sides of length 2*a* and a crack of length *a* is used (Fig. 6). The displacement fields for a mode 1 crack are (Anderson 1991)

$$u_x=\frac{K_1}{2\mu}\sqrt{\frac{r}{2\pi}}\cos\left(\frac{\theta}{2}\right)\left[\kappa-1+2\sin^2\left(\frac{\theta}{2}\right)\right] \tag{24a}$$

$$u_y=\frac{K_1}{2\mu}\sqrt{\frac{r}{2\pi}}\sin\left(\frac{\theta}{2}\right)\left[\kappa+1-2\cos^2\left(\frac{\theta}{2}\right)\right] \tag{24b}$$

where r is the distance from the crack tip and θ is the angle measured from the line of the crack. The stress intensity factor is prescribed as $K_1=1psi\sqrt{in}$. The stresses resulting from this displacement field satisfy the equilibrium and the solution is exact if the displacement from above Eqs. (24) are prescribed on the outer boundaries.

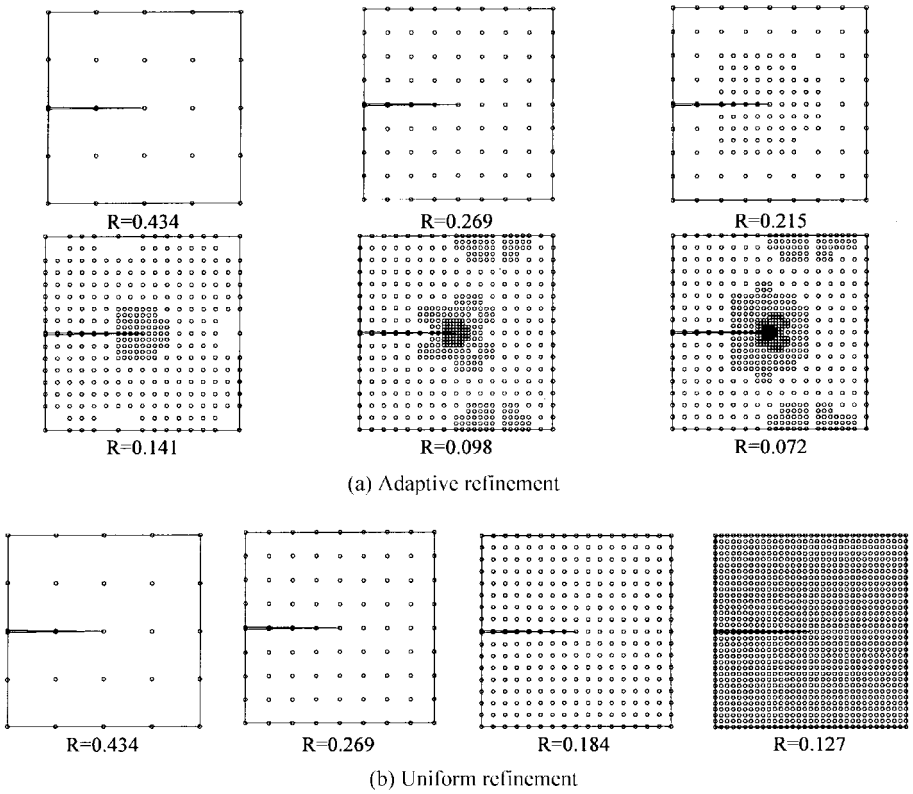

Fig. 7 Analysis sequences with relative error for example 2

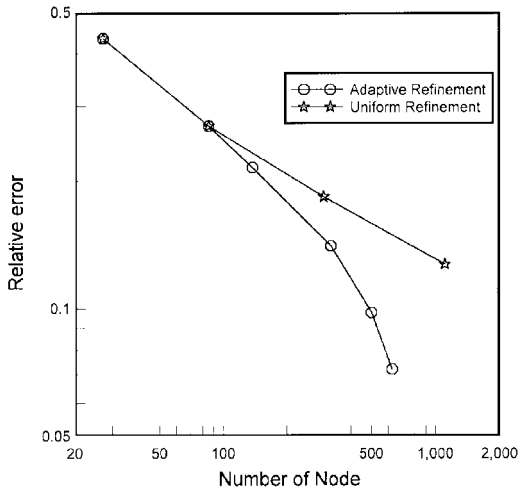

Fig. 8 Convergence curves for example 2

The problem is analyzed with D_m^a=2.5 and D_m^p=1.75. The value of error indicator that is used for the criteria of cell refinement is 0.1 for each iteration and the target level of relative error is 10%.

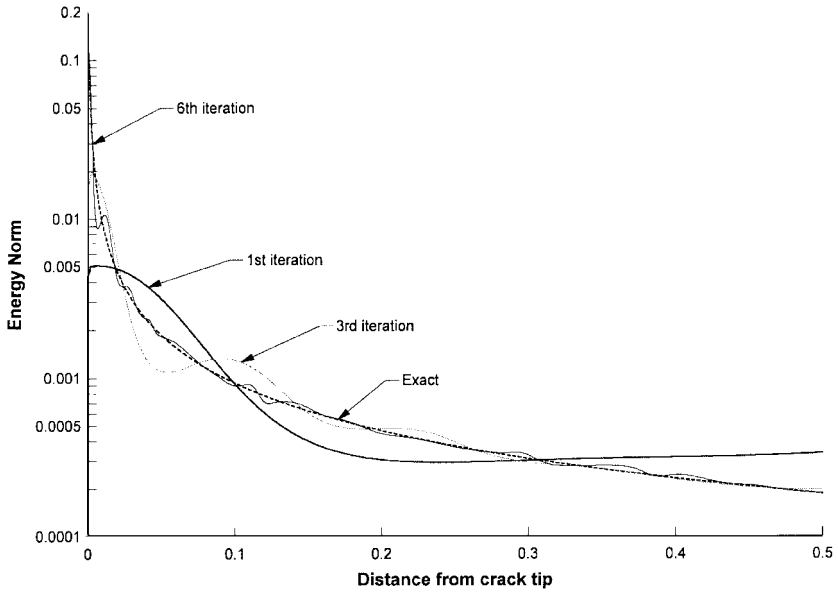

Fig. 9 Comparison of energy norm distributions along the *x* axis for example 2

The Fig. 7 shows refinement sequence of adaptive analysis model and analysis models of uniform refinement. As the previous example, new nodes are added around the crack tip in adaptive procedure. The distribution of added nodes resembles that of estimated error. The convergence ratio of adaptive analysis model and uniform refined model are compared in the Fig. 8. This figure shows the effectiveness of adaptive analysis. The recalculated value of K_1 at final step has 0.19% error for adaptive analysis and 2.37% error for uniformly refined analysis. In Fig. 9 distributions of energy norm along the x axis with different iteration step are compared.

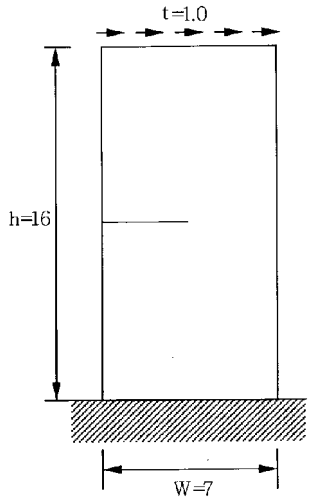

Fig. 10 Shear edge crack problem

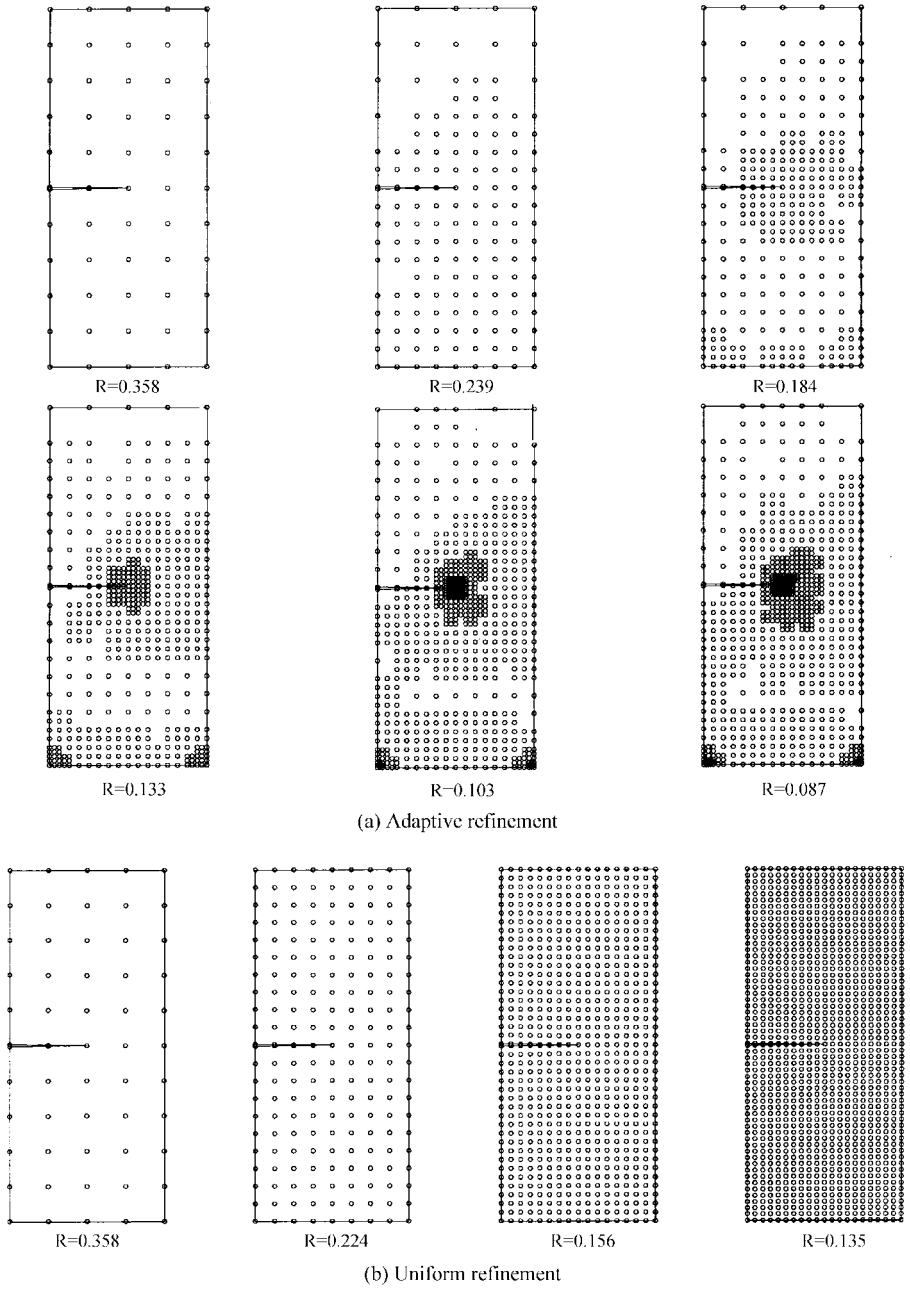

Fig. 11 Analysis sequences with relative error for example 3

4.3. Example 3: Shear edge crack

In this example, a plate subjected to shear traction τ=1.0 on the top and containing an edge crack of length a=W/2=3.5 is considered (see Fig. 10). The plate is clamped on the bottom. The material

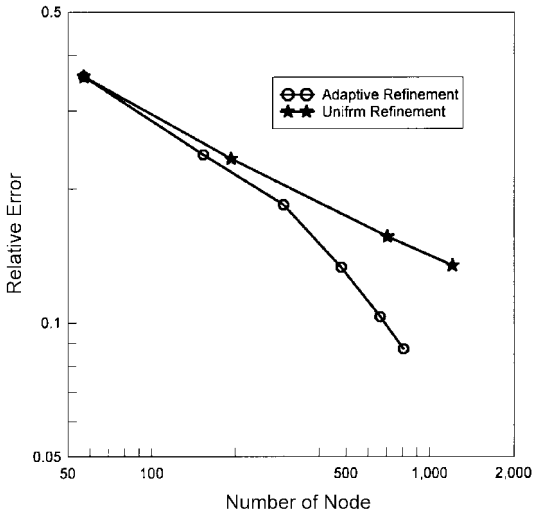

Fig. 12 Convergence curves for example 3

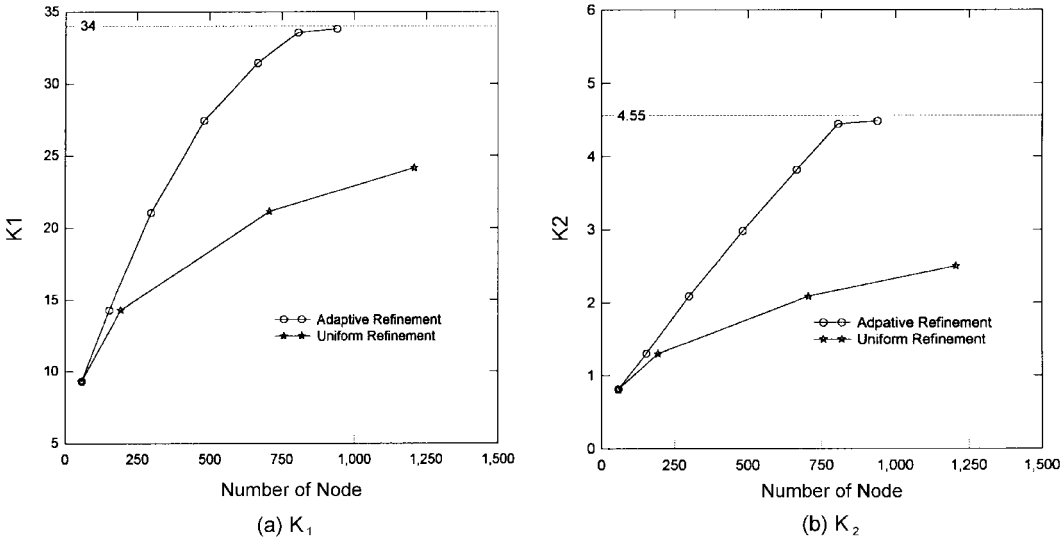

Fig. 13 Stress intensity factors

constants used are E=30.E6 and ν=0.25 and plane strain conditions are assumed. The stress intensity factors used for the reference solution are K_1=34.0 and K_2=4.55.

The problem is analyzed with D_m^a=2.5 and D_m^p=1.8. The value of error indicator that is used for a criterion of cell refinement is 0.15 for each iteration and the target level of relative error is 10%.

The adaptive and uniform refinement sequences are denoted Fig. 11 and convergence curves of this example is shown in Fig. 12. The variations of two stress intensity factors K_1 and K_2 along the analysis sequences are displayed in Fig. 13. In Fig. 14 distributions of Von-Mises stresses for initial and final nodal configuration which comes from adaptive procedure are presented .

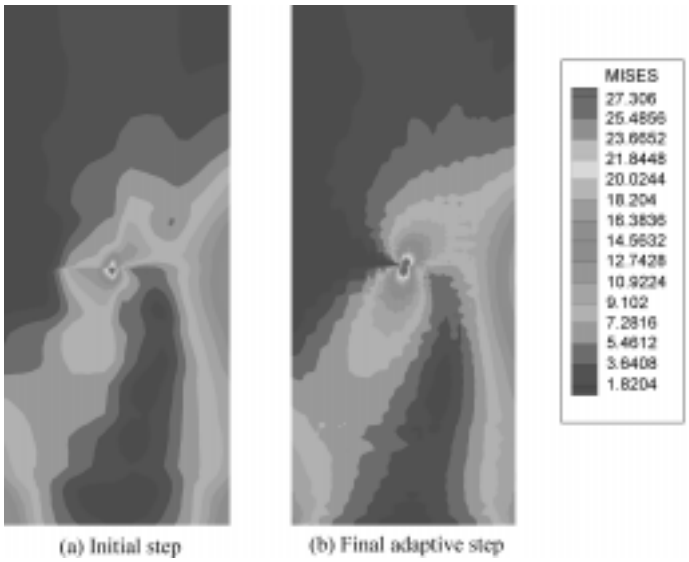

Fig. 14 Von-Mises stress distribution

5. Conclusions

The local and global error estimates for the element-free Galerkin (EFG) method and the adaptive refinement procedure using background integration cell are proposed. The point-wise errors are obtained by comparing the projected stresses and EFG stresses. This stress projection scheme requires no matrix solution procedure, which are needed in many other error estimation procedures.

To demonstrate the efficiency of proposed schemes, the adaptive refinement analyses are performed for several numerical examples. The convergence rates of adaptive refinement analysis are superior over those of uniform refinement analysis. Also the results of analysis show a high accuracy for structural parameters such as stress intensity factors.

From the aforementioned results, the strong possibility of *h*-type adaptivity of EFG method can be found. Since only one level refinement is carried out at each step of procedure, re-analyses are needed until the solution satisfies the desired accuracy. A more efficient refinement procedure need to be found to get a completely new nodal configuration which satisfies all user defined tolerance optimally.

A more sophisticated nodal generation method that is independent from the background structure and similar to bubble meshing technique will be presented in out next paper.

Acknowledgements

A part of this work (Heung-Jin Chung) was supported by Electrical Engineering and Science Research Institute and Jeonju University.

References

Anderson, T.L. (1991), *Fracture Mechanics: Fundamentals and Applications* (First ed.), CRC press.

Belytschko, T., Lu, Y.Y. and Gu, L. (1994), "Element-free Galerkin methods", *International Journal for Numerical Method in Engineering* **37**, 229-256.

Belytschko, T., Krongauz, Y., Fleming, M., Organ, D. and Liu, W.K. (1996a), "Smoothing and accelerated computations in the element-free Galerkin method", *Journal of Computational and Applied Mathematics*, **74**, 111-126.

Belytschko, T., Krongauz, Y., Organ, D., Fleming, M. and Krysl, P. (1996b), "Meshless methods: An overview and recent developments", *Computer Methods in Applied Mechanics and Engineering*, **139**, 3-47.

Chang-Koon Choi, Sun-Hoon Kim, Yong-Myung Park, and Keun-Young Chung (1998), "Two-dimensional Nonconforming finite elements: A state-of-the-art", *Structural Engineering and Mechanics, An International Journal*. **6**(1), 41-61.

Chang-Koon Choi and Won-Jin Yu, (1999), "Adaptive mesh refinement and recovery using variable-node element for finite element wind analysis", *Journal of Aerospace Engineering*, **12**(2), 168-175.

Chang-Koon Choi and Yong-Myung Park (1997), "Conforming and Nonconforming Transition Plate Bending Elements for an Adaptive h-refinement", *Thin-Walled Structures*, **28**(1), 1-20.

Duarte, C.A. and Oden, J.T. (1996), "An *hp* adaptive method using clouds", *Computer Methods in Applied Mechanics and Engineering*, **139**, 237-262.

Lancaster, P. and Salkauskas, K. (1981), "Surface generated by moving least squares method", *Math. Comput.*, **37**, 141-158.

Liu, W.K., Hao, W., Chen, Y., Jun, S. and Gosz, J. (1996), "Multiresolution reproducing kernel particle methods", *Computational Mechanics*, submitted.

Nayroles, B., Touzot, G. and Villon, P. (1992), "Generalizing the finite element method: diffuse approximation and diffuse elements", *Computational Mechanics*, **10**, 307-318.

Organ, D., Fleming, M., Terry, T. and Belytschko, T. (1996), Continuous meshless approximations for nonconvex bodies by diffraction and transparency*m Computational Mechanics* **18**(3), 225-235.

Timoshenko, S.P. and Goodier, J.N. (1970), *Theory of Elasticity* (Third ed.), McGraw Hill, New York.

Zienkiewicz, O.C. and Zhu, J.Z. (1987), "A simple error estimator and adaptive procedure for practical engineering analysis", *International Journal for Numerical Method in Engineering* **24**, 337-357

Chung,, H.J. and Belytschko, T. (1998), "An error estimate in the EFG method." *Computational Mechanics*, **21**, 91-110.

Hausser-Combe, U. and Korn, C. (1998), "An adaptive approach with the EFG method", *Computer Methods in Applied Mechanics and Engineering*, **162**, 203-222.